Pergamon

Geochimica et Cosmochimica Acta, Vol. 67, No. 23, pp. 4457–4469, 2003

0016-7037/03 $30.00 + .00

doi:10.1016/S0016-7037(03)00388-0

Kinetics and mechanism of polythionate oxidation to sulfate at low pH by O_2 and Fe^{3+}

GREGORY K. DRUSCHEL,[1,]* ROBERT J. HAMERS,[2] and JILLIAN F. BANFIELD[1,2]†
[1]Departments of Geology and Geophysics and
[2]Chemistry, University of Wisconsin-Madison, Madison, WI 53706 USA

(*Received October* 16, 2002; *accepted in revised form May* 30, 2003)

Abstract—Polythionates ($S_xO_6^{2-}$) are important in redox transformations involving many sulfur compounds. Here we investigate the oxidation kinetics and mechanisms of trithionate and tetrathionate oxidation between pH 0.4 and pH 2 in the presence of Fe^{3+} and/or oxygen. In these solutions, Fe^{3+} plus oxygen oxidizes tetrathionate and trithionate at least an order of magnitude faster than oxygen alone. Kinetic measurements, coupled with density functional calculations, suggest that the rate-limiting step for tetrathionate oxidation involves Fe^{3+} attachment, followed by electron density shifts that result in formation of a sulfite radical and $S_3O_3^0$ derivatives. The overall reaction orders for trithionate and tetrathionate are fractional due to rearrangement reactions and side reactions between reactants and intermediate products. The pseudo-first order rate coefficients for tetrathionate range from 10^{-11} s^{-1} at 25°C to 10^{-8} s^{-1} at 70°C, compared to 2×10^{-7} s^{-1} at 35 °C for trithionate. The apparent activation energy (E_A) for tetrathionate oxidation at pH 1.5 is 104.5 ± 4.13 kJ/mol. A rate law at pH 1.5 and 70°C between 0.5 and 5 millimolar [Fe^{3+}] is of the form:

$$r = 10^{-6.61\pm0.3}[S_4O_6{}^{2-}]^{0.3\pm0.08}[Fe^{3+}]^{0.15\pm0.09}$$

where rate, r, is in units of mol L^{-1} s^{-1}. In pH <1 solutions where trithionate forms by rearrangement of tetrathionate, trithionate oxidation is the rapid pathway for conversion of tetrathionate to sulfate. The kinetics of both trithionate and tetrathionate oxidation are several orders of magnitude slower than the formation of polythionates from thiosulfate in acidic, Fe^{3+}-rich solutions. *Copyright © 2003 Elsevier Ltd*

1. INTRODUCTION

Polythionates ($S_xO_6^{2-}$), also known as polysulfane disulfonic acids or polysulfane disulfonates, are sulfur-based molecules in which a sulfur chain is terminated at both ends by SO_3^- groups. These compounds are important intermediate species in the redox transformations of sulfur compounds in many environments and in the metabolism of sulfur-oxidizing and sulfur-reducing microorganisms (Chambers and Trudinger, 1979; Steudel et al., 1987; Kelly, 1999; Schippers et al., 1999; Suzuki, 1999; Takano et al., 2000; Xu et al., 2000).

Figure 1 represents an energy-minimized geometry for the trithionate molecule, $S_3O_6^{2-}$, tetrathionate molecule, $S_4O_6^{2-}$, and pentathionate molecule, $S_5O_6^{2-}$. The calculated charges on each of the sulfur and oxygen atoms are also represented in Figure 1, illustrating that the central sulfurs are more reduced than the terminal sulfurs. The central S-S bond is shorter than the two symmetrical S-S bonds involving the terminal sulfurs bonded to the oxygens. The bond lengths compare well with those determined by X-ray diffraction studies of polythionate salts (Christidis et al., 1989). Williamson and Rimstidt (1992) predicted the pK_2 of $H_2S_4O_6$ to be −2.3, indicating that these species are generally unprotonated at all but the most extreme pH values (Nordstrom et al., 2000).

As shown in the Eh-pH diagram (Fig. 2), polythionates have predominance fields intermediate between those of sulfide and sulfite (diagram produced by suppressing sulfate). Polythionates vary in chain length greatly, and contain up to 80 sulfurs in sulfur sols (Lyons and Nickless, 1968), up to 45 in synthetic compounds (Ancutiene and Janickis, 2000), and up to 22 sulfurs in bacterial sulfur excretions (Steudel et al., 1987).

Complex mixtures of polythionates are formed by the reaction of H_2S and SO_2, sometimes referred to as Wackenroeders solutions (Lyons and Nickless, 1968). In these solutions, polythionate chain length is generally governed by the equilibrium:

$$S_xO_6^{2-} + S_2O_3^{2-} \leftrightarrow S_{x+1}O_6^{2-} + SO_3^{2-} \tag{1}$$

Chain lengthening reaction is favored at pH <7, the pK_2 of sulfurous acid (H_2SO_3, Moses et al., 1987). Although theoretically polythionates can form very long chains, most are observed to have x = 3 to 6. The relative abundances of tetrathionate, trithionate, and pentathionate are governed by rearrangement reactions such as:

$$2\ S_4O_6^{2-} \leftrightarrow S_3O_6^{2-} + S_5O_6^{2-} \tag{2}$$

(Lyons and Nickless, 1968). Transformation of polythionate species can be either through redox reactions or through bimolecular nucleophilic displacement (S_N2, Moses et al., 1987). Additionally, polythionates undergo a hydrolysis reaction:

$$S_xO_6^{2-} + H_2O \rightarrow S_{x-1}O_3^{2-} + SO_4^{2-} + 2\ H^+ \tag{3}$$

$$S_xO_6^{2-} + y\ H_2O \rightarrow (0.58x)\ S_8 + (0.42x)\ SO_4^{2-} + (0.5\ H^+y) \tag{4}$$

(Meyer and Ospina, 1982). Some of the proposed products of polythionate reactions include the polysulfane monosulfonic acids (Steudel et al., 1987). These have the general formula $S_xO_3^{2-}$ and consist of chains of sulfur atoms terminated at one

---

* Author to whom correspondence should be addressed, at College of Marine Studies, University of Delaware, Lewes, DE 19958, USA (druschel@udel.edu).

† *Present address:* Department of Earth and Planetary Sciences, University of California, Berkeley, CA 94720, USA.

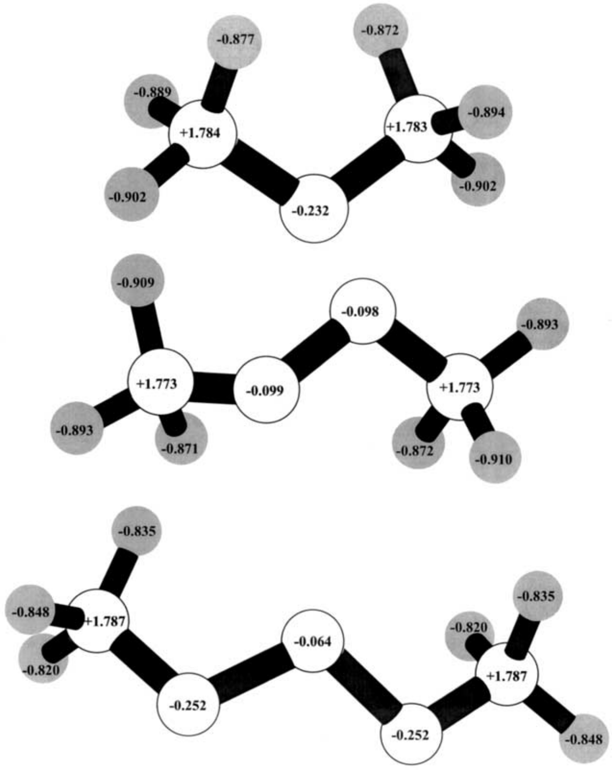

Fig. 1. Geometry optimized structure and natural charges of S and O in the lower polythionate species tri-, tetra-, and pentathionate, as calculated with gaussian98 employing B3LYP density functional theory using an LANL2DZ basis set.

end by an SO_3^- group. Polysulfane monosulfonic acids are also susceptible to nucleophilic displacement reactions resulting in chain lengthening/shortening:

$$S_xO_3^{2-} + S_2O_3^{2-} \rightarrow S_{x+1}O_3^{2-} + SO_3^{2-} \quad (5)$$

Similar reactions resulting in terminal sulfur oxidation form polythionate species and polysulfide (S_n^{2-}):

$$S_xO_3^{2-} + S_2O_3^{2-} \rightarrow S_xO_6^{2-} + S_2^{2-} \quad (6)$$

(Meyer and Ospina, 1982).

The work of Takano and Watanuki (1988) includes the only known preliminary assessment of the stability of tetrathionate in acidic solutions containing Fe^{3+}. Aside from noting sufficient stability in cold acidic solutions, these authors did not attempt to address either the mechanism or the kinetics of oxidation of this species.

Recent advances in the sampling and analysis (Druschel et al., 2003; for review, see O'Reilly et al., 2001) of polythionates have facilitated their direct identification and study in many environments. In a thermal spring in Yellowstone National Park, Xu et al. (2000) reported polythionate formation via thiosulfate oxidation in the presence of pyrite and polythionate decomposition either by reaction with H_2S or through hydrolysis. Polythionates have been detected within sulfur globules in a crater lake (Takano et al., 1994) and as part of the structure of microbially formed sulfur globules (Steudel et al., 1987). Changes in polythionate concentrations through reaction with aqueous SO_2 and H_2S discharged through vents may serve as an indicator of imminent volcanic eruptions (Takano, 1987).

The oxidation of metal sulfide minerals generates acidic, metal rich fluids. At many locations worldwide, mining of pyrite (FeS_2)-rich deposits has increased oxidative dissolution and led to formation of environmentally damaging solutions known as acid mine drainage (AMD). Figure 3 illustrates a general picture of some of the major pathways through which pyritic sulfur may oxidize in the environment (based on Goldhaber, 1983; Luther, 1987; Moses et al., 1987; Schippers et al., 1996; Nesbitt et al., 1998; Hu, 2002), based on how the pyritic sulfide dissociates from the pyrite to either oxygenated or nonoxygenated forms. Thiosulfate, $S_2O_3^{2-}$, has been proposed to be a leaving group in the oxidation of pyrite, based on experimental results and molecular orbital theory (Goldhaber, 1983; Luther, 1987; Moses et al., 1987). Subsequent oxidation of thiosulfate to either polythionates or elemental sulfur and sulfite has been determined experimentally by several groups (Johnston and McAmish, 1973; Williamson and Rimstidt, 1993; Xu and Schoonen, 1995). Observations of pyrite oxidation in experimental and natural settings have shown more thiosulfate and polythionate at circumneutral pH than at low pH (Goldhaber, 1983; Moses et al., 1987; Schippers and Sand, 1999; Elberling et al., 2000). This difference in reaction products must be due to either changes in the reactivity of those products in differing environments or to changes in reaction mechanism(s) and subsequent changes in pyrite oxidation pathways. The reactivity of polythionates at low pH is thus an important part of understanding the governing pathways of pyrite oxidation under different conditions. Several researchers have characterized polythionate reactions in the absence of iron (Meyer and Ospina, 1982; Steudel et al., 1987), and Schippers et al. (1996) suggested pyrite oxidation pathways including tetrathionate oxidation via hydrolysis reactions similar to reaction 3. However no attempts have yet been made towards defining reactivity of polythionates with Fe^{3+}.

It is the goal of this paper to investigate the oxidation of trithionate and tetrathionate to sulfate with Fe^{3+} in acidic solutions. We focus on their reactivity with Fe^{3+} because this species is abundant and important in many low pH environments. Transition metals including iron have been shown to influence the mechanism and kinetics of hydrogen sulfide, thiosulfate, sulfite, and polysulfide reactions (Williamson and Rimstidt, 1994; Brandt and Eldik, 1998; Millero, 2001). Thus, iron is expected to impact trithionate and tetrathionate reactivity.

2. MATERIALS AND METHODS

2.1. Kinetics Experiments

The kinetic investigation of polythionate oxidation was primarily carried out as batch reactions, utilizing ion chromatographic and spectroscopic determination of intermediate species. All experiments were carried out at pH between 0.4 and 2.

Potassium tetrathionate salts were obtained from Sigma (>99.9% purity), and sodium trithionate salts were synthesized after the method in Kelly and Wood (1994) utilizing the reaction of thiosulfate with hydrogen peroxide. Purity of the trithionate salt was determined by gravimetry and chromatographic analyses to be greater than 99%. Solutions of sulfide, thiosulfate, dithionate, and sulfite were prepared from appropriate salts under a nitrogen atmosphere immediately before use as chromatographic standards, and sulfate chromatographic stan-

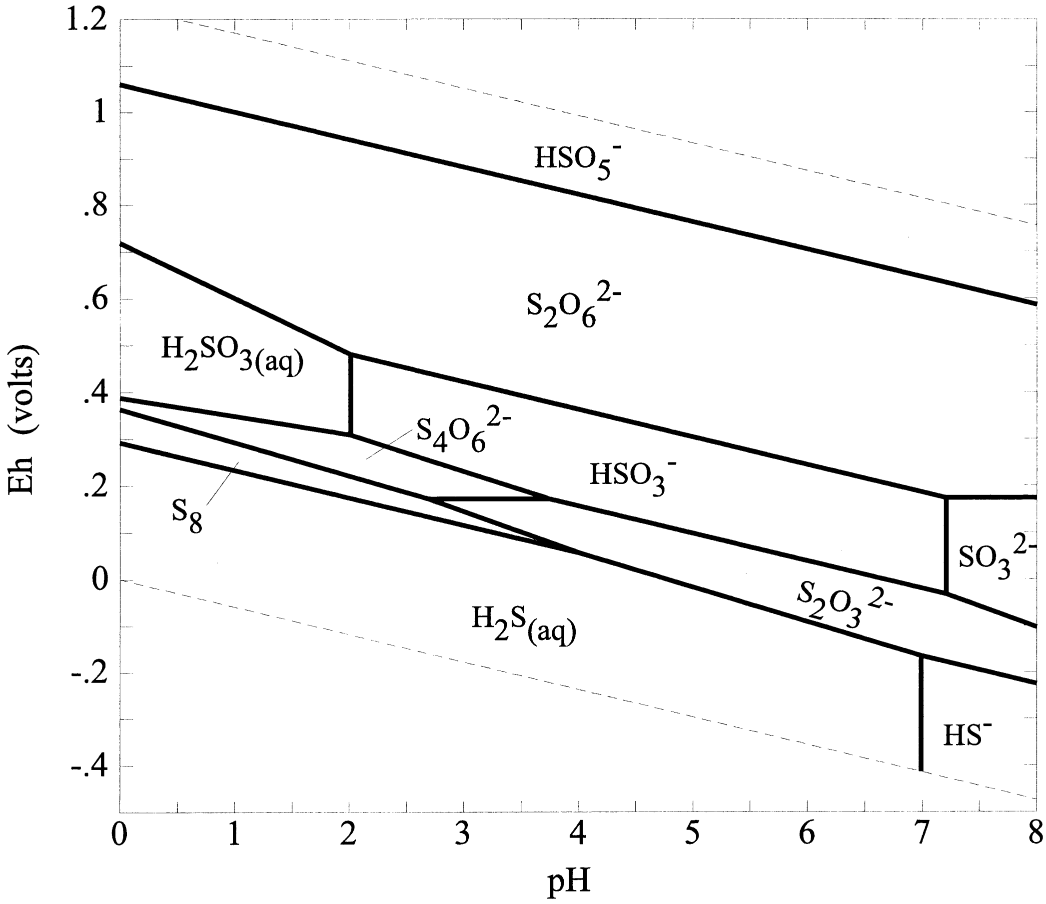

Fig. 2. Eh-pH diagram of intermediate sulfur species at 25°C, activity $\Sigma S = 1 \times 10^{-3}$ calculated with the Geochemist's Workbench (Bethke, 2000) and using the LLNL v6 r8 database.

dards were prepared from NIST-certified stock solution (FisherBrand). Fe^{3+} and Fe^{2+} stock solutions were prepared from chloride salts obtained from Sigma (ACS reagent grade) and stored in 0.5 mol/L HCl to minimize Fe^{2+} oxidation and maintain Fe^{3+} solutions at conditions undersaturated with respect to ferric oxyhydroxides. Elemental sulfur HPLC standards were prepared from EM Science sublimated S_8 powder, 99% minimum assay dissolved in 100% ACS grade perchloroethylene. All stock solutions were filter sterilized. Experimental solutions were prepared from normalized HCl (FisherBrand certified 1 N HCl solution), diluted with 18 MΩ nanopure H_2O, and spiked with the appropriate stock solutions when in the reaction vessel.

Tetrathionate formation from thiosulfate oxidation was studied by spiking 1 mM $S_2O_3^{2-}$ in 50 mL of 0.05 mol/L HCl solution with 1 mM $FeCl_2$ in a 125 mL glass septum bottle sealed with a rubber stopper to minimize any loss of gaseous sulfur species possibly evolved in the reaction progress. Duplicate experiments were conducted with 90% Fe^{2+} 10% Fe^{3+} and 10% Fe^{2+}, 90% Fe^{3+}. Samples were withdrawn after several minutes and after several hours to identify the products of this reaction.

Batch reactions for tetrathionate oxidation experiments were carried out in 125 mL glass septum bottles and sealed with rubber stoppers to minimize any loss of gaseous sulfur species possibly evolved in the reaction progress. Fifty mL experimental solutions were prepared and poured into the bottles, leaving oxygenated headspace with 10–100 times as much oxygen as could possibly be utilized by any reactions. The bottles were stoppered, placed in water baths at temperature, and sampled periodically through the rubber stopper with a needle and 3 mL syringe. Temperature profiles were performed to show that thermal equilibration of the solutions occurs in a matter of minutes. Two mL aliquots were withdrawn in time, with 1.5 mL transferred to 1.5 mL Eppendorf tubes, capped, and stored in a 4°C refrigerator for sulfur species analysis, and 0.5 mL used for immediate Fe^{2+} analysis. Several samples were analyzed by IC immediately to check the efficiency of the storage and low-temperature quenching of reaction progress. It was found that storage of the solutions over several days did not result in significant change of the reactant products for the tetrathionate experiments.

Multiple sets of experiments with different $[S_4O_6^{2-}]_{initial}$, $[Fe^{3+}]$, pH, ionic strength, and T were performed. Table 1 lists each of the experimental sets reported in this work and the principle variable studied in each, with all experimental conditions listed. Experimental sets investigating $[S_4O_6^{2-}]_{initial}$ and $[Fe^{3+}]$ dependence were corrected to equal ionic strength by the addition of KCl. For every experiment, a control was run without added Fe^{3+} to assess the contribution of thermal degradation and reaction with O_2 at the same pH and temperature conditions.

Trithionate experiments were originally carried out in the same manner, but it was found that the trithionate was much more reactive at lower temperature and therefore quenching and storage of collected aliquots was not possible. A 1-L, 3-port glass reaction vessel was utilized for the trithionate experiments. The vessel, containing 500 mL of solution at the desired pH and Fe^{3+} concentration, was allowed to equilibrate at temperature and a 1 mL spike of trithionate stock was added to begin the reaction. The solution was pumped directly from the reaction vessel with a single piston HPLC pump (Dionex DX10) directly into the sample loop of the ion chromatograph. The sample was then directly injected and analyzed at different time intervals by the chromatographic techniques described below. The vessel was left open to air through an open Teflon tube used to sample the solution for Fe^{2+}

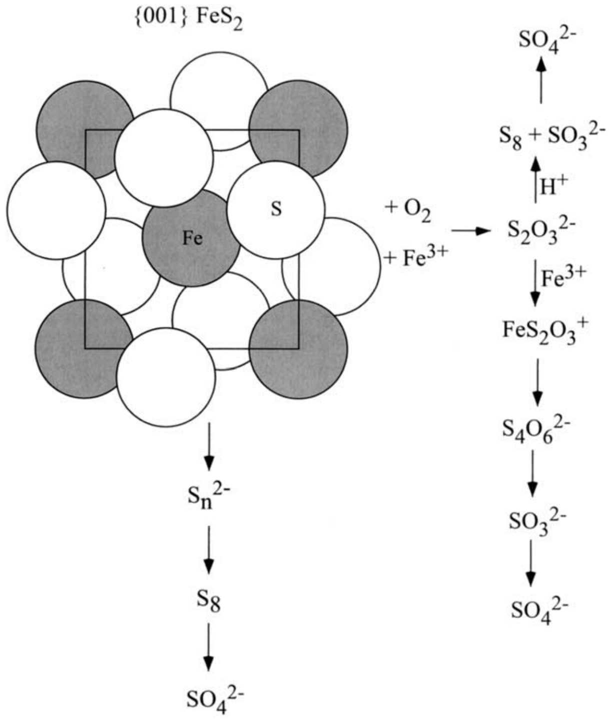

Fig. 3. Generalized diagram of some of the ideas possibly governing pyrite oxidation, (after Goldhaber, 1983; Luther, 1987; Moses et al., 1987; Schippers et al., 1996; Nesbitt et al., 1998; Hu, 2002).

analysis, except for a duplicate experiment that was constantly purged with argon.

2.2. Sample Characterization

Chromatographic analysis of collected aliquots for tetrathionate experiments was performed on a Dionex Series 500 ion chromatograph equipped with a conductivity detector and UV-Vis detector collected at 230 nm. Sulfate, sulfite, thiosulfate, dithionate, and sulfide were detectable using an isocratic 5mM $NaHCO_3$/5 mM Na_2CO_3 eluent at a 1.0 mL/min flow rate through an IonPac AS16 column. All peaks except sulfate were detectable with the UV-Vis detector. Polythionates were detected using an isocratic 30% acetonitrile:H_20 eluent containing 2 mM tetrabutylammonium hydroxide, buffered with 3 mM $NaHCO_3$/3 mM Na_2CO_3 and run through an IonPac NS1 column. The method was modified from Zou et al. (1993). Tri-, tetra-, and pentathionate were all resolvable down to 5 μM concentrations using a 25 μL sample loop.

Elemental sulfur was analyzed by HPLC using a Shimadzu system UV-Vis at 254 nm, an Alltech C18 column, and an isocratic 95% methanol:H_2O eluent at 1.0 mL/min after the method of McGuire and Hamers (2000).

Fe^{2+} was analyzed using 1,10 phenanthroline, and total iron was analyzed using a ferrozine method on a Hach model 2010 portable datalogging spectrophotometer.

2.3. Kinetic Analysis

Rate coefficients were calculated using a method of initial velocities (Brezonik, 1993). Reported rates are rates of tetrathionate degradation unless otherwise noted, and were calculated with the first 3–6 data points, depending on individual data set and best-fit statistics and is reported in units of mol L^{-1} s^{-1}. Using $\log r = \log k + n \log C$, $\log r$ vs. $\log C$ was plotted to determine rate coefficients (k's) and reaction orders (values of n) with respect to the changing concentrations of Fe^{3+}, initial tetrathionate, and ionic strength, respectively (after Rimstidt and Newcomb, 1993). For all experiments, pH and O_2 concentrations were held constant throughout. Apparent activation energy and collision frequency were calculated using the Arrhenius relationship. Fitting errors were calculated by determining the standard error of the mean from the regression fit using SigmaPlot 4.0. Errors were typically on the order of 5–15%, but were as high as 40% in some experiments. Deviations beyond standard analytical error (which is between 2 and 5% for chromatographic runs) are likely to be the result of complexity in the reaction pathway (Brezonik, 1993). Multiple linear regression of data sets for determination of an overall rate law was accomplished with the MINITAB Statistical Software package Minitab 13.32 (Minitab Inc., 2003). Multiple linear regression of several data sets at once is possible mathematically, but graphical representation with log-log plots would be in multidimensional space and is therefore not represented visually.

2.4. Calculations

Understanding of the geometry, electronic structure, and electron density shifts as a result of Fe^{3+} interaction was accomplished with several computational techniques. Chem3D (Version 5.0, CambridgeSoft Scientific Computing, Inc.) was used to assemble polythionates, polysulfane monosulfonic acids, and Fe^{3+} complexes, and the geometry was initially minimized using the molecular mechanics algorithm MM2. The z-matrix of the resulting molecule was output into a gaussian input file and run using gaussian98 (Frisch et al., 2001) on the computational cluster at the University of Wisconsin Department of Chemistry. All species were calculated in a spherical continuum with a dielectric constant of 80 (equivalent to water at 25°C) employing B3LYP density functional theory and the LANL2DZ basis set. Local charge densities were calculated using Natural Bond Orbital 5.0 (Glendening et al., 2001). Models were visualized using Molden3.7 (Schaftenaar and Noordik, 2000) with the gaussian98 output for each molecule.

An Eh-pH diagram showing predominance fields of intermediate sulfur species was calculated using the Geochemist's Workbench 3.1 (Bethke, 2000), suppressing sulfate as a species. The Lawrence Liver-

Table 1. List of tetrathionate experiments reported in this work, listing pertinent experimental conditions and the reaction variable investigated in each. The Series designation is used throughout the text for reference to these conditions.

Series	Reaction variable	Conditions
I	Rearrangement reaction	500 μM $S_4O_6^{2-}$ in 0.01, 0.05, 0.1 M HCl at 25°C 500, 1000, 2000, 5000 μM $S_4O_6^{2-}$ in 0.1 HCl at 25°C 500 μM $S_4O_6^{2-}$in 0.1 M HCl at 4, 25, 42, 70°C all open to oxygenated headspace, no Fe^{3+} present
II	O_2	500 μM $S_4O_6^{2-}$ in 0.05 M HCl and 2 mM Fe^{3+} at 25 and 70°C open to oxygenated headspace or Ar or N_2^{-} purged
III	Fe^{2+}, Zn^{2+}, Cu^+	500 μM $S_4O_6^{2-}$ in 0.05 M HCl and 2 mM Fe^{3+}, Zn^{2+}, or Cu^+ at 70°C open to oxygenated headspace
IV	[$S_4O_6^{2-}$] initial	120, 250, 500, 1000, or 2000 μM $S_4O_6^{2-}$ in 0.05 M HCl and 2 mM Fe^{3+} at 70°C open to oxygenated headspace
V	[Fe^{3+}] initial	500 μM $S_4O_6^{2-}$in 0.05 M HCl and 0.5, 1, 5, or 10 mM Fe^{3+} at 70°C open to oxygenated headspace
VI	Ionic strength	500 μM $S_4O_6^{2-}$in 0.5 M HCl and 1 mM Fe^{3+} at 70°C open to oxygenated headspace with 0.1, 0.25, 0.5, 1, or 2 M KCl added
VII	Temperature	1000 μM $S_4O_6^{2-}$ in 0.05 M HCl and 1 mM Fe^{3+} at 4, 25, 60, or 70°C open to oxygenated headspace

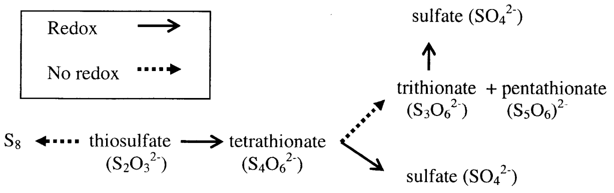

Fig. 4. Basic structure of experiments performed in this study. No redox reactions refer to reactions studied where there was no overall oxidation (or reduction) of the sulfur.

more National Labs V8 R6+ "combined" thermodynamic data set was utilized for all calculations.

Kinetic simulations of reactions of thiosulfate in acidic solutions utilized the Chemical Kinetics Simulator v 1.01 (available from IBM research at: www.almaden.ibm.com/st/msim/). Rate laws for individual reactions were input and the starting concentrations of reactants set to approximate experimental conditions.

3. RESULTS

The following section describes a series of experiments designed to follow the production of tetrathionate from thiosulfate and determine its fate via both rearrangement reactions and as the result of oxidation by Fe^{3+} and O_2 to sulfate. An outline for the experiments described below is shown in Figure 4.

3.1. Tetrathionate Formation at Low pH in the Presence of Excess Fe^{3+}

Reaction products of thiosulfate in acidic, Fe^{3+} rich solutions consisted of primarily tetrathionate. Tetrathionate production is consistent regardless of the presence of Fe^{2+} in solution at pH 1.5 as long as excess Fe^{3+} is present (data not shown). PCE extraction and analysis by HPLC showed that no measurable elemental sulfur was produced.

3.2. Tetrathionate Rearrangement to Trithionate and Pentathionate

Investigation of the nonoxidative reactivity of tetrathionate species under the relevant pH and temperature conditions was necessary before examination of the oxidation reactions. Table 2 lists the results of Series I experiments, where the ratio of trithionate to tetrathionate is expressed as the measure of reaction progress according to Eqn. 2. Xu et al. (2000) noted a solution of polythionates at pH = 1.0 equilibrated to a 15:70:15 mix trithionate, tetrathionate, and pentathionate after ~80 min, from a starting solution containing ~5% trithionate and pentathionate and 90% tetrathionate. Based on this, samples were measured after approximately 90 min of reaction, and did not change significantly in the following 24 h.

The rearrangement reaction does not appreciably occur within several days at pH >~ 1.0 (0.1 mol/L HCl), and is minimally affected by temperature between 25 and 70 °C. The extent of rearrangement does change as a function of $[S_4O_6^{2-}]_{initial}$. This result indicates rearrangement is not the result of a direct bimolecular reaction. The dependence of rearrangement on $[S_4O_6^{2-}]_{initial}$ could be due to reaction between polythionates and thiosulfate or sulfite, which may occur as minor impurities in the tetrathionate salt.

Table 2. Results of tetrathionate rearrangement reactions under different conditions expressed as the ratio of trithionate to tetrathionate and the ratio of trithionate to tetrathionate to pentathionate.

HCl (M)	$S_4O_6^{2-}$ initial concentration (μM)	T (°C)	$S_3O_6^{2-}/S_4O_6^{2-}$	$S_3O_6^{2-}:S_4O_6^{2-}:S_5O_6^{2-}$
0.01	500	25	0.0	0:100:0
0.05	500	25	0.0	0:100:0
0.05	500	70	0.0	0:100:0
0.1	500	25	0.45	22:56:22
0.1	1000	25	0.45	23:54:23
0.1	2000	25	0.39	19:62:19
0.1	5000	25	0.27	13:74:13
0.1	500	4	0.45	22:56:22
0.1	500	25	0.47	24:52:24
0.1	500	42	0.47	24:52:24
0.1	500	60	0.50	25:50:25

3.3. Tetrathionate Oxidation by Fe^{3+} and O^2

A number of possible reactants and principle variables have been tested for their role in the overall oxidation kinetics of tetrathionate to sulfate in the presence of Fe^{3+} at low pH (Table 1).

Intermediate species such as H_2S, $S_2O_6^{2}$, $H_2SO_{3(aq)}$, $HS_2O_3^{-}$, $S_3O_6^{2-}$, $S_4O_6^{2-}$, and $S_5O_6^{2-}$ would be identified by the techniques employed in the tetrathionate batch experiments if they persist in solution for even a few minutes. The only species typically identified by chromatographic analyses were $S_3O_6^{2-}$, $S_4O_6^{2-}$, $S_5O_6^{2-}$, and SO_4^{2-} (Fig. 5). In samples analyzed immediately, very small concentrations of $H_2SO_{3(aq)}$ (detected as sulfite) were occasionally observed, but this is rapidly converted to sulfate. Mass balance calculations indicate that all of the sulfur in these experiments is accounted for by these species. Analysis of sulfate as a principle reaction progress variable is therefore appropriate under these conditions.

Results of experiments executed under nitrogen or argon

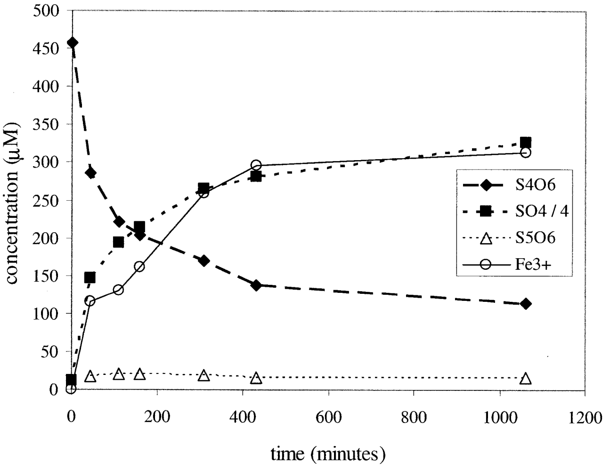

Fig. 5. Tetrathionate oxidation experiment with 500 μM $S_4O_6^{2-}$5 mM Fe^{3+} 70°C pH 1.5 (adjusted with HCl) open to O_2.

Table 3. Series IV experiments conducted to determine the order of reaction with respect to initial tetrathionate concentrations. Time-concentration data are in Table A1.

$[S_4O_6^{2-}]_{initial}$	120 μM	250 μM	500 μM	1000 μM	2000 μM
Initial rates (mol L^{-1} sc^{-1})	-1.31×10^{-8}	-1.40×10^{-8}	-1.89×10^{-8}	-2.43×10^{-8}	-2.47×10^{-8}

purge in the presence of Fe^{3+} show that both Fe^{3+} and oxygen are required to generate appreciable sulfate. Series II experiments N_2- or Ar-purged solutions showed a marked lack of reactivity over several days compared to identical solutions containing oxygen.

Series III experiments showed no evidence for catalysis of tetrathionate oxidation by their metal species over several days(data not shown).

Series IV experiments are presented in Table 3 and Table A1. Figure 6 plots log rate vs. log initial tetrathionate concentration. The reaction order with respect to the initial tetrathionate concentration, derived from the slope of the line, is approximately 0.3.

Series V experiments are presented in Table 4 and Table A2. Control experiments without Fe^{3+} oxidized ~ 10 times slower under identical conditions. The samples that contained the highest Fe^{3+} concentrations (5 and 10 mM Fe^{3+}) formed trithionate and pentathionate. In contrast, samples with lower Fe^{3+} concentrations only formed tetrathionate. The concentration of trithionate and pentathionate was not more than 10% of the total polythionate concentration for these experiments. The reaction order of tetrathionate degradation was found to be fractional with respect to Fe^{3+} concentration (Fig. 7). Similarly, the reaction order calculated for SO_4^{2-} generation from this reaction (normalized to 4 S species) was also found to be fractional. Figure 7 also plots the degree of imbalance (plotted as the difference between calculated rates for tetrathionate degradation and sulfate generation for the reaction, normalized to equivalent sulfurs). This imbalance should be a measurement of species not accounted for between these end members. Most analyses are within the analytical uncertainty for the methods used.

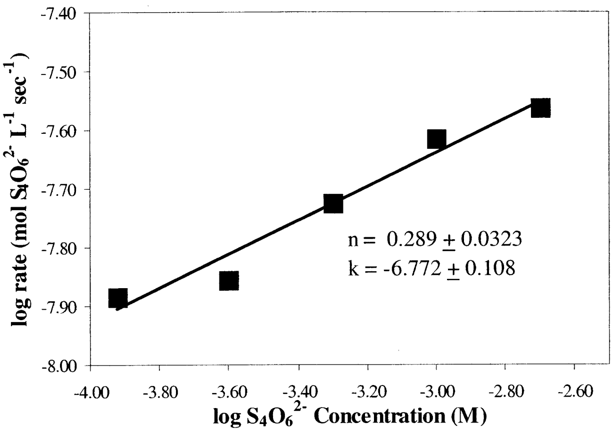

Fig. 6. - Log-log plot of initial rate of Series IV experiments vs. log variable $[S_4O_6^{2-}]_{initial}$, with 2 mM Fe^{3+}, pH 1.5, at 70°C (rate data available in Table 3 and Table A1).

The amount of Fe^{2+} produced may be used as an indicator of the relative roles of Fe^{3+} and oxygen as oxidants in the conversion of tetrathionate to sulfate. It is reasonable to assume that Fe^{2+} is not reoxidized by oxygen because this reaction is very slow at $pH<2$ (Singer and Stumm, 1970). In numerous experiments, including those shown in Figures 6 and 11, the Fe^{2+}:$S_xO_6^{2-}$ molar ratio ranged between 1:1 and 4:1.

Series VI experiments are presented in Table 5 and Table A3. Initial rates were determined between two initial points over 45 min of reaction. The plot of log initial rate vs. $I^{1/2}$ (Bronsted relationship, see Brezonik, 1993) yields a slope of -0.5 (Fig. 8). As ionic strength increases, the initial slope decreases whereas the total rates (over 30 h of reaction time) show an independence with respect to ionic strength.

Series VII experiments are presented in Table 6 and Table A4. An Arrhenius plot (Fig. 9) of log initial rates vs. 1/T yields an apparent activation energy of 104.5 ± 4.13 kJ/mol, with a calculated preexponential factor of 9.5×10^{11} J mol^{-1}.

3.4. Trithionate Oxidation Results

The rate of trithionate oxidation exhibits an initial reaction rate of 2×10^{-7} mol L^{-1} s^{-1} (Fig. 10). Under continual argon purging the oxidation rate was significantly slower than in identical experiments with atmospheric oxygen. Only sulfate and minor amounts of sulfite were produced (no thiosulfate, sulfide, other polythionates, or elemental sulfur were detected).

4. DISCUSSION

To predict the importance of tetrathionate production in oxidizing systems that contain thiosulfate, we carried out kinetic simulations using the rates for thiosulfate disproportionation in acidic solutions to yield elemental sulfur and sulfite:

$$S_2O_3^{2-} + H^+ \rightarrow S^0 + HSO_3^- \tag{7}$$

(Johnston and McAmish, 1973) and thiosulfate oxidation by Fe^{3+} to form tetrathionate:

Table 4. Results of Series V experiments conducted to determine the order of reaction with respect to initial Fe^{3+} concentrations. $SO_4^{2-}/4$ is the sulfur-normalized formation rate, determined by dividing the SO_4^{2-} initial rate by four. Time-concentration data are in Table A2.

$[Fe^{3+}]$ initial (μM)	$S_4O_6^{2-}$ initial rate (mol L^{-1} s^{-1})	SO_4^{2-} initial rate (mol L^{-1} s^{-1})	$SO_4^{2-}/4$ initial rate (mol L^{-1} s^{-1})
500	-1.52×10^{-8}	3.72×10^{-8}	9.29×10^{-9}
1000	-2.40×10^{-8}	6.73×10^{-8}	1.68×10^{-8}
5000	-2.48×10^{-8}	7.85×10^{-8}	1.96×10^{-8}
10,000	-1.82×10^{-8}	6.00×10^{-8}	1.5×10^{-8}

Table 5. Results of Series VI experiments conducted to examine the dependence of the rate of polythionate oxidation at pH 0.5 on ionic strength. Time-concentration data are in Table A3.

M KCl	Initial rate (mol L^{-1} s^{-1})	Total rate (mol L^{-1} s^{-1})
0.1	-4.70×10^{-8}	-2.45×10^{-9}
0.25	-4.59×10^{-8}	-2.36×10^{-9}
0.5	-3.92×10^{-8}	-2.32×10^{-9}
1	-2.24×10^{-8}	-3.16×10^{-9}
2	-1.48×10^{-8}	-2.36×10^{-9}

$$2\ S_2O_3^{2-} + 2\ Fe^{3+} \rightarrow 2\ FeS_2O_3{+} \rightarrow S_4O_6^{2-} + 2\ Fe^{2+} \quad (8)$$

(Williamson and Rimstidt, 1993).

Kinetic simulations (Fig. 11) under low pH conditions show that the reaction of thiosulfate with Fe^{3+} in solution (reaction 8) is much faster than disproportionation (reaction 7), and in acidic solutions containing excess Fe^{3+}, almost 100% of thiosulfate produced by oxidation of pyrite would form tetrathionate. Experimental results also show that tetrathionate is produced from thiosulfate instead of elemental sulfur and sulfite in low pH solutions containing excess Fe^{3+}. This result reflects the general case made by Williamson and Rimstidt (1993) that in the presence of excess Fe^{3+}, tetrathionate should be the predominant product of thiosulfate oxidation. The result is also consistent with the results of Schippers et al. (1996).

In pH 1 solution, tetrathionate rearrangement to trithionate and pentathionate (Series I experiments) yields a $S_3O_6^{2-}$/$S_4O_6^{2-}$ratio of ~0.5 for 500 μM $S_4O_6^{2-}$starting concentrations. Assuming the pentathionate concentration is equal to the trithionate concentration (Eqn. 2), the ratio of $S_3O_6^{2-}$: $S_4O_6^{2-}$: $S_5O_6^{2-}$ would be approximately 25:50:25. At higher concentrations of initial $S_4O_6^{2-}$, the degree of tetrathionate rearrangement is less (Table 2). Xu et al. (2000) note a rearrangement ratio of 15:70:15 for a 500 μM $K_2S_4O_6$ salt which contained approximately 5% $S_3O_6^{2-}$ and $S_5O_6^{2-}$ impurity at pH 1. The discrepancy between the results of Xu et al. (2000) and this study is probably due to differences in the concentrations of other sulfur compounds in the starting salts.

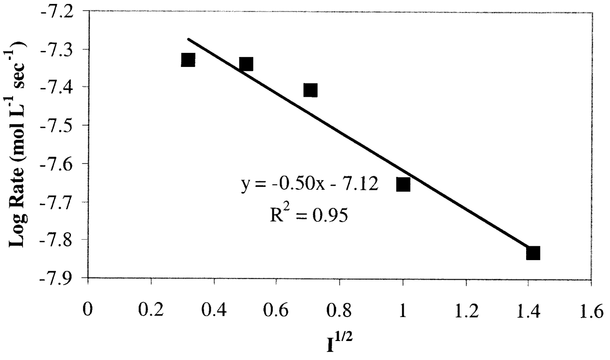

Fig. 8. Dependence of tetrathionate decomposition rates on ionic strength (I) in Series VI experiments. After the Bronsted equation, relating ionic strength to kinetics, the negative slope indicates reaction between oppositely charged species where greater ionic strength effectively shields the range of electrostatic interaction.

Table 6. Results of Series VII experiments conducted to determine the temperature dependence of tetrathionate oxidation at pH 1.5. Time-concentration data are in Table A4.

Temperature (°C)	Initial rate (mol L^{-1} s^{-1})
25	5.67×10^{-11}
45	2.92×10^{-9}
60	1.08×10^{-8}
70	2.73×10^{-8}

4.1. Products of Tetrathionate Oxidation by Fe^{3+} and O^2

Intermediate sulfur products of tetrathionate oxidation by Fe^{3+} must be stable in these solutions for at least several minutes to be detected by the methods employed. Thus, our analyses are unable to detect a subset of possible intermediates (e.g., dithionates, and sulfoxyanion radicals). Sulfite was observed in minor quantities in several experiments, but was oxidized completely within several minutes after initial detection, which is consistent with prior experiments (Brandt and Eldik, 1998). Elemental sulfur was not observed in any of the experiments. This result implies that polysulfides were not produced because polysulfides polymerize into elemental sulfur at these conditions (Luther, 1990; Hu, 2002). Trithionate and pentathionate were observed as intermediate products of tetrathionate oxidation at a pH high enough that their formation would not be due to the rearrangement reaction. These species may be due to side reactions similar to those illustrated in Eqn. 1, where the reaction of tetrathionate with sulfite or thiosulfate yields trithionate and pentathionate. However, thiosulfate and sulfite are so reactive in these solutions that they are unlikely to persist long enough to participate in reactions with tetrathionate. Thus, the trithionate and pentathionate products are probably the result of reactions involving polysulfane monosulfonic acids (see Eqns. 5 and 6, after Steudel et al., 1987, and Meyer and Ospina, 1982).

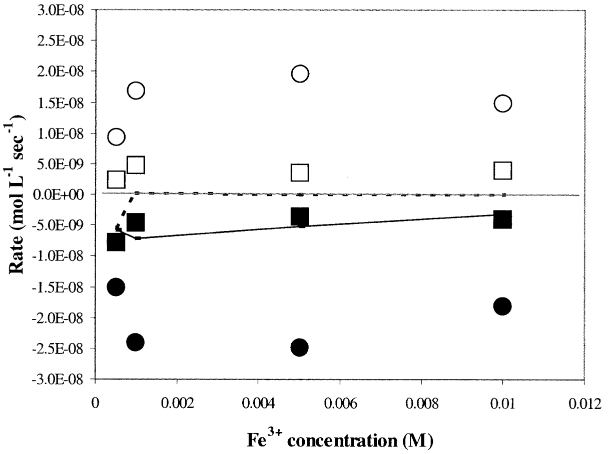

Fig. 7. Comparison of calculated rates for Series V experiments. Lines indicate the difference between rates calculated for directly measured $S_4O_6^{2-}$(solid markers) and SO_4^{2-} (open markers). Round markers are rates calculated from initial rates while square markers are calculated from total rates. $S_4O_6^{2-}$rates were normalized to 1 sulfur.

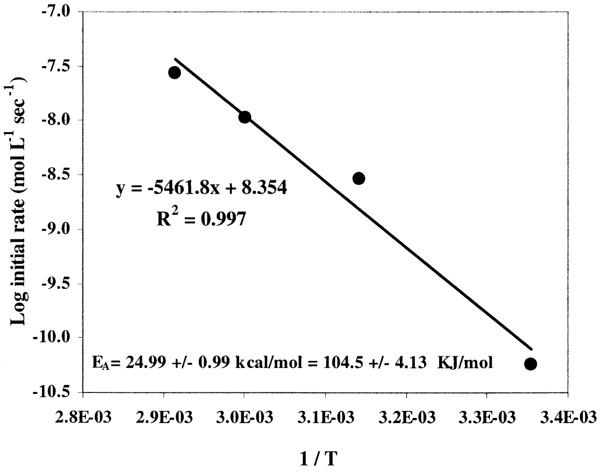

Fig. 9. Arrhenius plot showing the apparent activation energy for the Series VII experiments.

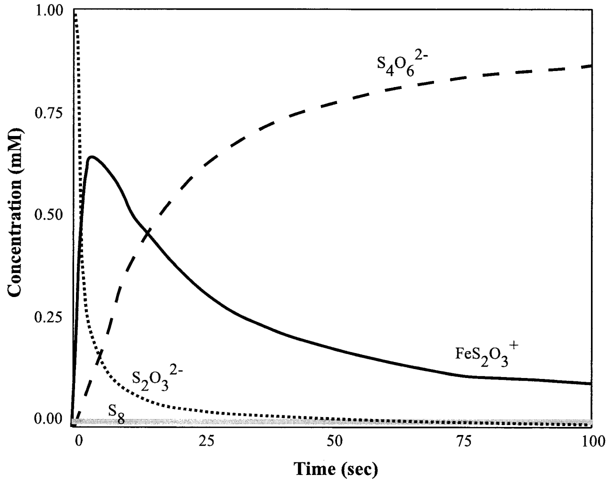

Fig. 11. Results of kinetic calculations for the fate of 1000 μM thiosulfate in a pH 1.5 solution containing 2 mM Fe^{3+}. Note that negligible S_8 was formed as a result of disproportionation in this solution and that ~100% of the thiosulfate is converted to tetrathionate. Rate laws from Johnston and McAmish (1973) and Williamson and Rimstidt (1993) were used in this calculation.

4.2. Fe^{3+} and O^2 as Oxidants in Tetrathionate and Trithionate Oxidation

Observation of the slower rate at which sulfoxyanion products form in the absence of O_2 and the molar ratio of Fe^{3+} as an electron donor in these experiments illustrate the role of O_2 in the overall reaction pathway (Series II, V experiments). The amount of Fe^{2+} generated is much less than that expected if Fe^{3+} is the sole oxidant. Thus, oxygen is a more efficient oxidant of some intermediate products between tetrathionate and sulfate than Fe^{3+}. Because species such as thiosulfate and sulfite are more efficiently oxidized by Fe^{3+} compared to O_2, this result suggests that polysulfane monosulfonic acids and sulfur radicals are in integral part of the reaction pathway.

The kinetics of Fe^{2+} generation correlates well with the degradation of $S_4O_6^{2-}$and $S_3O_6^{2-}$ (Figs. 5 and 10). Thus, Fe^{3+} is a direct participant in the oxidation of these polythionates, even though it is not the only oxidant (see above). Over the pH range investigated, the Fe^{3+} in solution exists primarily as the hexaaquo complex $Fe(H_2O)_6^{3+}$. The slow rate of polythionate oxidation in the absence of Fe^{3+} suggests that Fe^{3+} is involved in the initial reaction step of the oxidation. Given the lack of significant concentrations of observed intermediates, this step is probably rate-limiting. This suggests that a $FeS_4O_6^+$ complex is a transition state towards the formation of polysulfane monosulfonic acids ($S_xO_3^{2-}$) and sulfite.

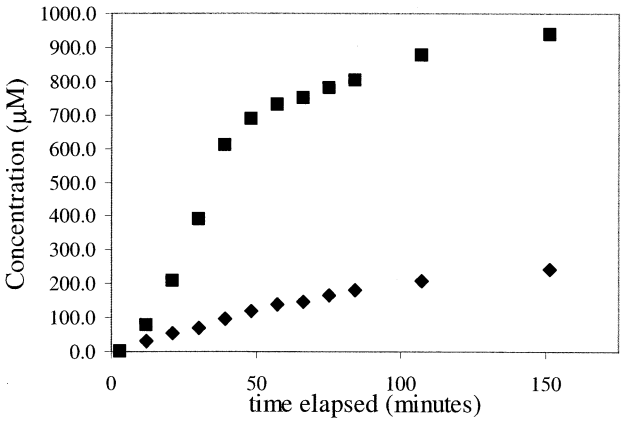

Fig. 10. Diagram of a trithionate oxidation experiment with 500 μM $S_3O_6^{2-}$ at 35°C in a pH 1.5 solution with 2 mM Fe^{3+}. The squares represent SO_4^{2-} and the diamonds represent Fe^{2+} measured in the course of the experiment.

It remains unclear from experimental results whether or not the transition state yields Fe^{2+}. It not, Fe^{3+} could be described as a catalyst (none of the other metal ions tested catalyzed tetrathionate oxidation). Regardless of whether or not the Fe^{3+} is a catalyst, the data clearly suggest that Fe^{3+} has an important role in the overall oxidation kinetics of tetrathionate.

The oxidation of polythionates in acidic solutions containing excess Fe^{3+} occurs by complex pathways containing many steps. Based on our experimental results, the overall reaction may be approximated:

$$S_4O_6^{2-} + 3\,Fe^{3+} + 2.75\,O_2 + 4.5\,H_2O \rightarrow 4\,SO_4^{2-} + 3\,Fe^{2+} + 9\,H^+ \quad (9)$$

The ratio of Fe^{3+} to oxygen consumed in experiments varied between 2:3 and 4:2.5 In the average case (reaction 9), 55% of the excess oxygen in sulfate is derived from O_2. In contrast, 70% of the excess oxygen in sulfate would be O_2-derived in a pathway that only utilized O_2 as the oxidant. This difference could be measured in future work.

4.3. Implications of the Dependence on [Fe^{3+}]

In the absence of an unlimited external supply of Fe^{3+}, the dependence of polythionate oxidation on Fe^{3+} means that the rate of Fe^{2+} reoxidation by oxygen could determine the rate at which sulfate is generated. At low pH, reoxidation of Fe^{2+} by O_2 is extremely slow. As has been pointed out previously (e.g., Singer and Stumm 1970), Fe-oxidizing microorganisms present in natural acidic environments accelerate Fe^{2+} oxidation rates by up to 5 orders of magnitude. Thus, the consequence of the dependence of polythionate oxidation rates on iron oxidation rates may be a dependence of the rate on microbial activity.

4.4. Role of Ionic Strength

Ionic strength was found to have an inverse effect on the initial rates of oxidation of tetrathionate at between 0.1 and 2 mol/L (Series VI experiments; Fig. 8). The slope of log k vs. $I^{1/2}$ is negative, consistent with reaction between oppositely charged species (Brezonik 1993). The Bronsted equation predicts this slope to be equivalent to the product of the charges between the reactants, and therefore reaction between Fe^{3+} and $S_4O_6^{2-}$may be expected to yield a slope of −6. The total rates of reaction exhibit a log k vs. $I^{1/2}$ slope of approximately zero (Table 5), indicating a greater influence on neutral species and like-charged interactions as the reaction progresses. The results qualitatively indicate that an electrostatic interaction between reactants is a part of the reaction pathway, and that reaction with neutral species may also be a significant part of the overall reaction pathway.

4.5. Relative Rates of Tetrathionate and Trithionate Oxidation

Tetrathionate and trithionate oxidation in low pH, oxygenated, Fe^{3+}-rich solutions is generally slow compared to reactions involving sulfide, thiosulfate, and sulfite. The rate of thiosulfate oxidation to tetrathionate in acidic, Fe^{3+}-rich solutions is many orders of magnitude faster than tetrathionate oxidation (Williamson and Rimstidt, 1993; Xu and Schoonen, 1995). Thus, tetrathionate should accumulate in solution.

The oxidation rate of trithionate is several orders of magnitude faster than that of tetrathionate under identical conditions throughout the range of temperatures, Fe^{3+} concentrations, and acidity investigated. Oxidation of tetrathionate below a pH of 1 is therefore controlled by the rearrangement reaction of tetrathionate to form trithionate.

4.6. $[Fe^{3+}]_0$, $[S_4O_6^{2-}]_0$, and $[H^+]$ Dependence of Tetrathionate Oxidation

The dependence of sulfate production on Fe^{3+} concentration is very complex. In almost all experiments (those conducted at $< \sim 2$ mM $[Fe^{3+}]$), the rate depends directly, but not linearly, on $[Fe^{3+}]$. This can be seen by comparison of initial rates for 0.5 mM and 1 mM $[Fe^{3+}]_{initial}$ and in the instantaneous rates within these experiments.

An intriguing feature of the results for oxidation of tetrathionate by Fe^{3+} is that the rate constant decreases with increasing $[Fe^{3+}]$ at very high initial $[Fe^{3+}]$ (Fig. 7). The explanation for the inverse dependence of the rate on $[Fe^{3+}]_{initial}$ is unclear, but may be due to rapid back reaction of S_2O_x species to yield tetrathionate at high $[Fe^{3+}]$ (e.g., reaction of thiosulfate to tetrathionate is very fast in the presence of Fe^{3+}).

Between pH 1 and 2, there is no measured dependence on $[H^+]$ on the oxidation rate. Solution pH <1 can influence the rate of sulfate production through conversion of tetrathionate to trithionate, while solution pH $> \sim 2$ limits $[Fe^{3+}]_{aq}$ due to precipitation of FeOOH. Multiple linear regression of tetrathionate oxidation rates measured over a range of concentrations (Tables 3 and 4) was used to investigate the dependence of rate on $[Fe^{3+}]_{initial}$ and $[S_4O_6^{2-}]_{initial}$ at pH 1 to 2 and 70°C. Results of multiple linear regression of the log values yields a rate law of:

$$r = 10^{-6.61 \pm 0.3}[S_4O_6^{2-}]^{0.3 \pm 0.08}[Fe^{3+}]^{0.06 \pm 0.07}$$

where the rate of sulfate production from tetrathionate oxidation, r, is in units of mol L^{-1} s^{-1}. Although the dependence of reaction rate on $[Fe^{3+}]_{initial}$ is not linear (Fig. 7), the rate of reaction varies more significantly with $[S_4O_6^{2-}]_{initial}$. The analysis shows a possible zero-order overall dependence on initial Fe^{3+}, but that is a function of a poor fit to nonlinear data. Removal of the highest value (10 mM Fe^{3+} experiment) in the regression yields an order of 0.15±0.09 for $[Fe^{3+}]$, illustrating the observed increase in rate in the presence of Fe^{3+}. This form of the rate law more accurately reflects the nature of the reaction, but caution must be exercised in applying the rate law to solutions containing iron outside the range used in these calculations.

4.7. Proposed Mechanism of Polythionate Oxidation

A mechanism for polythionate oxidation formed in the course of pyrite oxidation has been proposed by Schippers et al. (1996), based in part on hydrolysis reactions of polythionates to polysulfane monosulfonic acids and oxidation by molecular oxygen. Here we propose a mechanism independent of this, but one that should be considered as a potential parallel pathway in the oxidation of polythionates at low pH in the presence of excess Fe^{3+}.

Cleavage of the S-S bonds is critical in the overall oxidation of tetrathionate to sulfate. The central S-S bond or one of the two symmetrical terminal S-S bonds may be ruptured. Ab initio calculations of polythionate structures (this study) and X-ray diffraction studies of tetrathionate salts (Christidis et al., 1989) suggest that the terminal S-S bonds are longer and weaker in comparison to the inner S-S bond. Thus, the pathway is likely to favor terminal S-S cleavage reactions.

Calculations of the electronic structure of the $S_4O_6^{2-}$molecule (Fig. 1) show that breaking one of the terminal S-S bonds without electron density redistribution would yield $S_3O_3^-$ and SO_3^- (Fig. 12). Figure 12 illustrates the partial charge separation in the original $S_4O_6^{2-}$molecule and the calculated electron density for $FeS_4O_6^+$. Formation of the Fe^{3+} complex causes electrons to shift to Fe^{3+}, reducing it to Fe^{2+}. It is important to note that we were unable to obtain geometry optimization of the $FeS_4O_6^+$ molecule using optimization functions in the gaussian98 program. The molecular geometry was optimized using the molecular mechanics algorithm MM2 (contained in Chem3D) and imported to gaussian98, where only the energy was minimized.

Shifts in electron density towards the Fe^{3+} following formation of the $FeS_4O_6^+$ complex probably leads directly to rupture of a terminal S-S bond in tetrathionate (Fig. 13). The degree of electron shift across the S-S bond affects the charge distribution in the resulting species and can be represented by one of the following four reactions:

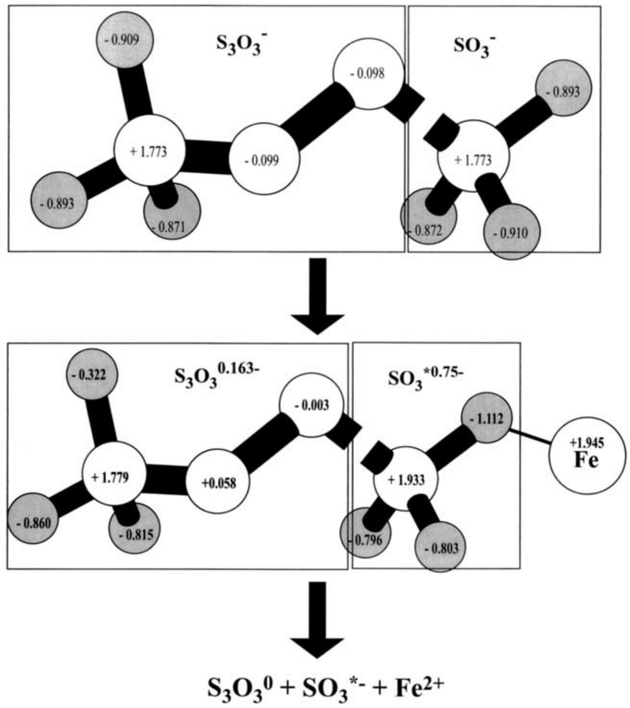

Fig. 12. gaussian98 calculations of tetrathionate and proposed transition state $FeS_4O_6^+$, illustrating the degree of electron density shift as a result of Fe^{3+}-complexation and cleavage of a terminal S-S bond.

$$S_4O_6^{2-} + Fe^{3+} \rightarrow S_3O_3^{2-} + SO_3^+ + Fe^{2+} \tag{10}$$

or

$$S_4O_6^{2-} + Fe^{3+} \rightarrow S_3O_3^- + SO_3^0 + Fe^{2+} \tag{11}$$

or

$$S_4O_6^{2-} + Fe^{3+} \rightarrow S_3O_3^0 + SO_3^{*-} + Fe^{2+} \tag{12}$$

or

$$S_4O_6^{2-} + Fe^{3+} \rightarrow S_3O_3^+ + SO_3^{2-} + Fe^{2+} \tag{13}$$

Formation of SO_3^+ via reaction 10 is highly unlikely because it would require S is in a +7 state (i.e., withdrawal of an electron from a filled 2p energy level). Formation of SO_3^0 is unlikely (reaction 11), as this would involve stripping of all valence electrons from S, resulting in $S^{VI}O_3^0$ (it is also unclear how this molecule might form SO_4^{2-} with no electrons left to covalently bond oxygen with). The ab initio results suggest that electron density shifts of the order of magnitude that would result in SO_3^{*-} (where * denotes a radical species) via reaction 10 are most plausible (Fig. 12). Formation of sulfite via reaction 13 would be possible if the degree of electron density shift is significantly greater than that predicted by the DFT model.

It is conceivable that $S_3O_3^0$ formed by reaction 10 could oxidize to $S_3O_6^{2-}$ via series of hydrolysis and oxidation reactions:

$$S_3O_3^0 + H_2O \rightarrow S_3O_4^{2-} + 2\ H^+ \tag{14}$$

$$S_3O_4^{2-} + O_2 \rightarrow S_3O_6^{2-} \tag{15}$$

$S_3O_3^0$ may also undergo chain-lengthening/shortening reactions (e.g., Eqn. 5) before oxidation of the terminal sulfur (sulfone) group (Eqn. 6, 14, and 15).

The mechanism of trithionate oxidation may be very similar to that for tetrathionate, e.g.,

$$S_3O_6^{2-} + Fe^{3+} \rightarrow S_2O_3^0 + SO_3^{*-} + Fe^{2+} \tag{16}$$

The $S_2O_3^0$ product may then undergo a series of hydrolysis and oxidation reactions to form SO_3^{*-} radicals (as postulated for $S_3O_3^0$ in Eqns. 14 and 15).

The SO_3^{*-} tetrathionate and trithionate oxidation product (Eqns. 12 and 16) is an accepted part of the chain mechanism commonly invoked for the oxidation of sulfite to sulfate (Ermakov, 1997). SO_3^{*-} will react very quickly to sulfate (Brandt and Eldik, 1998). A proposed overall reaction pathway, based on a combination of theoretical calculations and experimental results, is shown in Figure 13.

4.8. Kinetic Parameters and Implications for Pyrite Oxidation

The order of the tetrathionate and trithionate oxidation reactions is fractional and the rate exhibits a nonlinear dependence on Fe^{3+} concentrations. This is due in part to the complexity of the pathway, and specifically to the importance of side reactions and parallel reactions.

Oxidation rates of tetrathionate range between $10^{-11}\ s^{-1}$ at 25°C and $10^{-8}\ s^{-1}$ at 70°C (pseudo first order rate coefficients). The oxidation of trithionate exhibits a pseudo first order rate constant of $2 \times 10^{-7}\ s^{-1}$ at 35 °C. Because trithionate oxidation is several orders of magnitude faster than tetrathionate oxidation at comparable temperatures, trithionate oxidation should control overall tetrathionate oxidation rates at solution pH's <1 where rearrangement of tetrathionate to trithionate occurs.

The slow oxidation of polythionates in low pH solutions containing excess Fe^{3+} (which is many orders of magnitude slower than the formation of polythionates from thiosulfate) indicates that a pathway progressing through thiosulfate in these conditions should yield significant quantities of polythionates. However, this is not supported by experimental or field

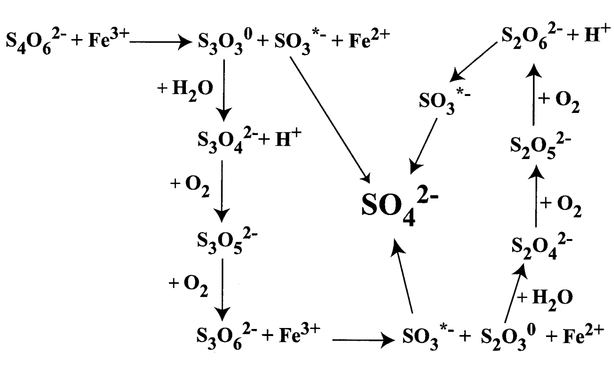

Fig. 13. Proposed pathway of tetrathionate oxidation at low pH in the presence of excess Fe^{3+}. This generalized pathway is proposed based on empirical observations and theoretical computational evidence.

observations of pyrite oxidation products in low pH environments containing significant concentrations of Fe^{3+} (Schippers et al., 1996; Druschel, 2002). At low pH, this brings into question the pathway for pyrite oxidation involving release of thiosulfate and the oxidation of dissolved thiosulfate by Fe^{3+} to form tetrathionate, followed by conversion of tetrathionate to sulfate (Fig. 3). Although the mechanism of formation of thiosulfate-like moieties on the pyrite surface may be valid over a wide range of pH conditions (Luther, 1987), the thiosulfate detachment step may not be favored at lower pH.

5. CONCLUSIONS

Trithionate and tetrathionate oxidizes with both Fe^{3+} and molecular oxygen to sulfate through an initial step in which formation of Fe^{3+}-polythionate complexes result in the break of a terminal S-S bond to form SO_3n- and polysulfane monosulfonic acids. The overall reaction of tetrathionate in oxic, low pH conditions with excess Fe^{3+} may be represented by:

$$S_4O_6^{2-} + 3\,Fe^{3+} + 2.75\,O_2 + 4.5\,H_2O \rightarrow 4\,SO_4^{2-} + 3\,Fe^{2+} + 9\,H^+ \qquad (9)$$

With both Fe^{3+} and molecular oxygen present in these reactions as potential oxidants, the competition for reduced species between them indicates some intermediates in the reaction pathway are more efficiently oxidized by one or the other. The proposed details of the reaction pathway (Fig. 13) are based on a combination of experimental and calculation results, and are consistent with oxygenation and charge balances in the transformation of polythionates to sulfate.

The rate law for the overall oxidation of tetrathionate to sulfate has been defined as fractional in order with respect to both Fe^{3+} and initial tetrathionate concentration In oxic, low pH conditions between 0.5 and 5 mM Fe^{3+} the rate law is:

$$r = 10^{-6.61 \pm 0.3}[S_4O_6^{2-}]^{0.3 \pm 0.08}[Fe^{3+}]^{0.15 \pm 0.09}$$

where the rate of sulfate production from tetrathionate oxidation, r, is in units of mol L^{-1} s^{-1}. This reaction of tetrathionate to sulfate is characterized by a high activation energy (104.5 ± 4.13 kJ/mol, with a calculated preexponential factor of 9.5×10^{11} J mol^{-1}), and a relationship of reaction rate with ionic strength that supports a reaction pathway rate-limited by an initial step involving oppositely charged species.

The reaction of trithionate is shown to be several orders of magnitude faster than tetrathionate oxidation under these conditions, implicating a fast reaction pathway for tetrathionate oxidation below pH 1 that may be through trithionate oxidation coupled with a rearrangement reaction.

The overall rates of tetrathionate and trithionate oxidation are markedly slower than rates of oxidation of thiosulfate (forming tetrathionate; Williamson and Rimstidt, 1993) in acidic, Fe^{3+}-rich solutions. This indicates that polythionates will persist in these environments where they form from thiosulfate, and thus may be metabolized by organisms that utilize intermediate sulfur compounds for energy generation. These kinetic data provide new insights into sulfur transformations under low pH conditions in the presence of excess Fe^{3+}.

Acknowledgments—We would like to thank Dr. Martin Schoonen and Michael Borda (State University of New York at Stony Brook), Dr. George Luther (University of Delaware), Dr. Bo Hu (University of Wisconsin), and Dr. Mark Williamson (Geochemical Solutions, CO) for very helpful suggestions and comments on this manuscript. This research was supported by grant CHE 9521731, CHE 9807598 from the National Science Foundation. We would also like to thank A. Schippers and two anonymous reviewers for their comments towards improving this manuscript, and to J.D. Rimstidt for editorial handling and a very valuable review.

Associate editor: D. Rimstidt

REFERENCES

Ancutiene I. and Janickis V. (2000) Chemical deposition of copper sulfide films in the surface of polyethylene by the use of higher polythionic acids. *Prog. Coll. Pol. Sci. S.* **116,** 129–133.

Bethke C. M. (2000) *The Geochemist's Workbench 3.1: A User's Guide to Rxn, Act2, Tact, React, and Gtplot.* University of Illinois.

Brandt C. and van Eldik R. (1998) Kinetics and mechanism of the iron(III)-catalyzed autooxidation of sulfur(IV) oxides in aqueous solution. The influence of pH, medium and aging. *Transit. Metal. Chem.* **23,** 667–675.

Brezonik P. L. (1993) *Chemical Kinetics and Process Dynamics in Aquatic Systems.* CRC Press.

Chambers L. A. and Trudinger P. A. (1979) Microbiological fractionation of stable sulfur isotopes: A review and critique. *Geomicrobiol. J.* **1,** 249–293.

Christidis P. C., Rentzeperis P. J., Kirfel A., and Will G. (1989) Experimental charge density in polythionate anions: II. X-ray study of the electron density distribution in potassium tetrathionate, $K_2S_4O_6$. *Z. Kristallogr.* **188,** 31–42.

Druschel G. K. (2002) Sulfur biogeochemistry. Kinetics of intermediate sulfur species reactions in the environment. Ph.D. thesis. University of Wisconsin.

Druschel G. K., Schoonen M. A. A., Nordstrom D. K., Ball J. W., Xu Y., and Cohn C. (2003) Sulfur geochemistry of hydrothermal waters in Yellowstone National Park, Wyoming, USA. II: An anion-exchange resin technique for sampling and preservation of sulfoxyanions in natural waters. *Geochem. Trans.* **4**(3), 12–19.

Elberling B., Schippers A., and Sand W. (2000) Bacterial and chemical oxidation of pyritic mine tailings at low temperatures. *J. Contam. Hydrol.* **41,** 225–238.

Ermakov A. N., Poskrebyshev G. A., and Purmal A. P. (1997) Sulfite oxidation: The state-of-the-art of the problem. *Kinet. Catal.* **38,** 295–308.

Frisch M. J., Trucks G. W., Schlegel H. B., Scuseria J. A., Robb M. A., Cheeseman J. R., Zakrzewski V. G., Montgomery J. A., Stratmann R. E., Burant J. C., Dapprich S., Millam J. M., Daniels A. D., Kudin K. N., Strain M. C., Farkas O., Tomasi J., Barone V., Cossi M., Cammi R., Mennucci B., Pomelli C., Adamo C., Clifford S., Ochterski J., Petersson G. A., Ayala P. Y., Cui Q., Morokuma K., Malick D. K., Rabuck A. D., Raghavachari K., Foresman J. B., Cioslowski J., Ortiz J. V., Stefanov B. B., Liu G., Liashenko A., Piskorz P., Komaromi I., Gomperts R., Martin R. L., Fox D. J., Keith T., Al-Laham M. A., Peng C. Y., Nanayakkara A., Gonzalez C., Challacombe M., Gill P. M. W., Johnson B., Chen W., Wong M. W., Andres J. L., Gonzalez C., Head-Gordon M., Replogle E. S., and Pople J. A. (2001) *Gaussian98* (Revision A.4). Gaussian Inc.

Glendening E. D., Badenhoop J. K., Reed A. E., Carpenter J. E., Bohmann J. A., Morales C. M., and Weinhold F. (2001) *NBO 5.0.*Theoretical Chemistry Institute.

Goldhaber M. B. (1983) Experimental study of metastable sulfur oxyanion formation during pyrite oxidation at pH 6–9 and 30 C. *Am. J. Sci.* **283,** 193–217.

Hu B. (2002) Chemical and structural study at the interface between metal sulfides and acids. Ph.D. thesis. University of Wisconsin.

Johnston F. and McAmish L. (1973) A study of the rates of sulfur production in acid thiosulfate solutions using S-35. *J. Colloid. Interf. Sci.* **42,** 112–119.

Kelly D. P. (1999) Thermodynamic aspects of energy conservation by chemolithotrophic sulfur bacteria in relation to the sulfur oxidation pathways. *Arch. Microbiol.* **171,** 219–229.

Kelly D. P. and Wood A. P. (1994) Synthesis and determination of thiosulfate and polythionates. In *Methods in Enzymology,*Vol. 243, *Inorganic Microbial Sulfur Metabolism* (eds. H. D. Peck Jr. and J. LeGall), pp. 475–501. Academic Press.

Luther G. W. III. (1987) Pyrite oxidation and reduction: Molecular orbital theory considerations. *Geochim. Cosmochim. Acta* **51,** 3193–3.

Luther G. W. III (1990) The frontier-molecular-orbital theory approach in geochemical processes. In *Aquatic Chemical Kinetics* (ed. W. Stumm), pp. 173–198. Wiley.

Lyons D. and Nickless G. (1968) The lower oxy-acids of sulphur. In *Inorganic Sulphur Chemistry* (ed. G. Nickless), pp. 509–534. Elsevier.

McGuire M. M. and Hamers R. J. (2000) Extraction and quantitative analysis of elemental sulfur from sulfide mineral surfaces by high-performance liquid chromatography. *Environ. Sci. Technol.* **34,** 4651–4655.

Meyer B. and Ospina M. (1982) Raman spectrometric study of the decomposition of aqueous tri- and tetrathionate. *Phosphorus Sulfur* **14,** 23–38.

Millero F. J. (2001) *The Physical Chemistry of Natural Waters.* Wiley.

Minitab Inc. (2003) *MINITAB User's Guide 2: Data Analysis and Quality Tools.* Release 13 for Windows.

Moses C. O., Nordstrom D. K., Herman J. S., and Mills A. L. (1987) Aqueous pyrite oxidation by dissolved oxygen and by ferric iron. *Geochim. Cosmochim. Acta* **51,** 1561–1571.

Nesbitt H. W., Bancroft G. M., Pratt A. R., and Scaint M. J. (1998) Sulfur and iron surface states on fractured pyrite surfaces. *Am. Min.* **83,** 1067–1076.

Nordstrom D. K., Alpers C. N., Ptacek C. J., and Blowes D. W. (2000) Negative pH and extremely acidic mine waters from Iron Mountain, California. *Environ. Sci. Technol.* **34,** 254–258.

O'Reilly J. W., Dicinoski G. W., Shaw M. J., and Haddard P. R. (2001) Chromatographic and electrophoretic separation of inorganic sulfur and sulfur-oxygen species. *Anal. Chim. Acta* **432,** 165–192.

Rimstidt J. D. and Newcomb W. D. (1993) Measurement and analysis of rate data: The rate of reaction of ferric iron with pyrite. *Geochim. Cosmochim. Acta* **57,** 1919–1934.

Schaftenaar G. and Noordik J. H. (2000) Molden: a pre- and post-processing program for molecular and electronic structures. *J. Comput. Aid. Mol. Des.* **14,** 123–134.

Schippers A., Jozsa P., and Sand W. (1996) Sulfur chemistry in bacterial leaching of pyrite. *Appl. Environ. Microb.* **62,** 3424–3431.

Schippers A., Rohwerder T., and Sand W. (1999) Intermediary sulfur compounds in pyrite oxidation: Implications for bioleaching and biodepyritization of coal. *Appl. Microbiol. Biot.* **52,** 104–110.

Schippers A. and Sand W. (1999) Bacterial leaching of metal sulfides proceeds by two indirect mechanisms via thiosulfate or via polysulfides and elemental sulfur. *Appl. Environ. Microb.* **65,** 319–321.

Singer P. C. and Stumm W. (1970) Acidic mine drainage: The rate-determining step. *Science* **167,** 1121–1123.

Steudel R., Holdt G., Gobel T., and Hazeu W. (1987) Chromatographic-separation of higher polythionates $SnO_6(2-)$ (n = 3. . .22) and their detection in cultures of thiobacillus-ferrooxidans—Molecular composition of bacterial sulfur secretions. *Angew. Chem. Int. Edit.* **26,** 151–153.

Suzuki I. (1999) Oxidation of inorganic sulfur compounds: Chemical and enzymatic reactions. *Can. J. Microbiol.* **45,** 97–105.

Takano B. (1987) Correlation of volcanic activity with sulfur oxyanion speciation in a crater lake. *Science* **235,** 1633–1635.

Takano B., Saitoh H., and Takano E. (1994) Geochemical implications of subaqueous molten sulfur at Yugama Crater Lake, Kusatsu-Shirane Volcano, Japan. *Geochem. J.* **28,** 199–216.

Takano B. and Watanuki K. (1988) Quenching and liquid chromatographic determination of polythionates in natural water. *Talanta* **35,** 847–854.

Takano B., Zheng Q., and Ohsawa S. (2000) A telemetering system for monitoring aqueous polythionates in an active crater lake. *J. Volcanol. Geoth. Res.* **97,** 397–406.

Williamson M. A. and Rimstidt J. D. (1992) Correlation between structure and thermodynamic properties of aqueous sulfur species. *Geochim. Cosmochim. Acta* **56,** 3867–3880.

Williamson M. A. and Rimstidt J. D. (1993) The rate of decomposition of the ferric-thiosulfate complex in acidic aqueous solutions. *Geochim. Cosmochim. Acta* **57,** 3555–3561.

Williamson M. A. and Rimstidt J. D. (1994) The kinetics and electrochemical rate-determining step of aqueous pyrite oxidation. *Geochim. Cosmochim. Acta* **58,** 5443–5454.

Xu Y. and Schoonen M. A. A. (1995) The stability of thiosulfate in the presence of pyrite in low-temperature aqueous solutions. *Geochim. Cosmochim. Acta* **59,** 4605–4622.

Xu Y., Schoonen M. A. A., Nordstrom D. K., Cunningham K. M., and Ball J. W. (2000) Sulfur geochemistry of hydrothermal waters in Yellowstone National Park, Wyoming, USA, II: Formation and decomposition of thiosulfate and polythionates in Cinder Pool. *J. Volcanol. Geoth. Res.* **97,** 407–423.

Zou H., Jia Z., Zhang Y., and Lu P. (1993) Separation of aqueous polythionates by reversed-phase ion-pair liquid chromatography with suppressor-conductivity detection. *Anal. Chim. Acta* **284,** 59–65.

APPENDIX

Table A1. Data for experiments investigating tetrathionate degradation rate dependence with [$S_4O_6^{2-}$] at pH 1.5, 70°C with 2 mM Fe^{3+}.

Time elapsed (min)	Initial [$S_4O_6^{2-}$]				
	120 μM	250 μM	500 μM	1000 μM	2000 μM
1	24	34	47	61	107
40	143	146	138	219	377
100	336	543	577	814	812
160	368	640	750	1064	1224
220	377	727	1009	1468	1457
280	454	867	1155	1592	2000
340	464	896	1342	1726	2279
475	474	1005	1484	2171	2854
595	454	na[a]	1605	2427	3015
715	485	na	1655	2522	3831
845	478	na	1694	2681	3663
1295	na	1045	1801	3034	4188

[a] na = not analyzed.

Table A3. Data for experiments investigating tetrathionate degradation rate dependence with ionic strength dependence (pH 0.5, 70°C, 500 μM $S_4O_6^{2-}$, 1000 μM Fe^{3+}).

Time elapsed (min)	Ionic strength (M KCl)				
	0.1 M	0.25 M	0.5 M	1 M	2 M
1	0	0	0	0	0
65	721	704	602	344	227
120	891	881	765	489	355
185	1023	1010	911	651	468
250	1160	1094	1015	794	565
330	1237	1156	1154	957	639
440	1331	1289	1240	961	na
570	1398	1383	1335	1082	862
690	1454	1414	1374	1111	912
825	1488	1463	1427	1294	969
935	na[a]	na	1452	na	na
1410	1580	1517	1608	1412	1180
1770	na	na	1653	na	1253

[a] na = not analyzed.

Table A2. Data for experiments investigating tetrathionate degradation rate dependence with [Fe^{3+}] at pH 1.5, 70°C, 500 μM $S_4O_6^{2-}$.

Time elapsed (min)	500 μM Fe^{3+}				1000 μM Fe^{3+}				5000 μM Fe^{3+}				10,000 μM Fe^{3+}			
	$S_3O_6^{2-}$ (μM)	$S_4O_6^{2-}$ (μM)	$S_5O_6^{2-}$ (μM)	SO_4^{2-} (μM)	$S_3O_6^{2-}$ (μM)	$S_4O_6^{2-}$ (μM)	$S_5O_6^{2-}$ (μM)	SO_4^{2-} (μM)	$S_3O_6^{2-}$ (μM)	$S_4O_6^{2-}$ (μM)	$S_5O_6^{2-}$ (μM)	SO_4^{2-} (μM)	$S_4O_6^{2-}$ (μM)	$S_5O_6^{2-}$ (μM)	$S_3O_6^{2-}$ (μM)	SO_4^{2-} (μM)
0	nd[a]	442	nd	16	nd	465	nd	33	nd	457	nd	47	446	nd	4	105
45	nd	370	nd	237	nd	330	nd	404	nd	286	17	589	310	6	16	497
110	nd	314	nd	341	nd	254	nd	627	nd	221	20	772	276	5	6	653
160	nd	294	nd	392	nd	227	nd	700	nd	203	20	858	254	nd	3	718
430	nd	216	nd	534	nd	203	nd	922	nd	170	19	1063	233	nd	nd	919
310	nd	na	nd	616	nd	131	nd	1190	nd	138	17	1125	176	2	nd	1070
1060	nd	na	nd	754	nd	89	nd	1451	nd	115	16	1305	114	nd	nd	1350

[a] nd = not detected.

Table A4. Data for experiments investigating tetrathionate degradation rate dependence with temperature at pH 1.5, 1000 μM $S_4O_6^{2-}$, 2000 μM Fe^{3+}.

25°C		45°C		60°C		70°C	
Total elapsed time (min)	SO_4^{2-} conc. (μM)	Total elapsed time (min)	SO_4^{2-} conc. (μM)	Total elapsed time (min)	SO_4^{2-} conc. (μM)	Time elapsed (min)	SO_4^{2-} conc. (μM)
0	0	0	0	0	0	1	61
380	10	380	368	380	847	40	219
1830	40	635	516	635	1664	100	814
3450	60	1460	978	1460	2243	160	1064
6545	90	2290	1683	1820	2426	220	1468
		3440	2030	2290	2529	280	1592
		4355	2224	2935	2622	340	1726
		5820	2442	3440	2695	475	2171
		7260	2492	4355	2756	595	2427
				5820	2890	715	2522
				7260	2948	845	2681
						1295	3034